Regulation of Soluble Neuropilin 1, an Endogenous Angiogenesis Inhibitor, in Liver Development and Regeneration

Dipak Panigrahy[1,2,5], **Irit Adini**[1,2], **Roni Mamluk**[1,2], **Nicholas Levonyak**[1], **Christiane J. Bruns**[7], **Patricia A. D'Amore**[3,4,6], **Michael Klagsbrun**[1,2,4], and **Diane R. Bielenberg**[1,2]

[1]Vascular Biology Program, Boston Children's Hospital

[2]Department of Surgery, Harvard Medical School

[3]Department of Ophthalmology, Harvard Medical School

[4]Department of Pathology, Harvard Medical School

[5]Center for Vascular Biology Research, Beth Israel Deaconess Medical Center

[6]Schepens Eye Research Institute, Massachusetts Eye & Ear; Boston, Massachusetts

[7]Department of Surgery, Klinikum Grosshadern, LMU Munich, Munich, Germany

Summary

Neuropilin-1 (NRP1) is a receptor for vascular endothelial growth factor (VEGF). A soluble isoform of Nrp1 (sNrp1) has not been described in the mouse. Our goal was to examine the expression of mouse sNrp1 during liver development and regeneration. sNrp1 was cloned from mouse liver. The expression of sNrp1 and VEGF was examined in mouse liver during postnatal development and regeneration using northern blot, western blot, *in situ* hybridization, and immunohistochemical analyses. HGF/NRP1 binding was examined *in vitro*. A novel 588-amino acid sNrp1 isoform was found to contain the ligand binding regions of Nrp1. The adult liver expressed more sNrp1 than full-length Nrp1. *In vivo*, hepatocytes constitutively expressed VEGF and sNrp1 in the quiescent state. *sNrp1* was highly upregulated at P20, a time point coinciding with a plateau in liver and body weights. Following hepatectomy, endogenous levels of *sNrp1* decreased during the rapid growth phase; and VEGF levels were highest just prior to and during the angiogenic phase. *sNrp1* levels again rose 5-10 days post-hepatectomy, presumably to control regeneration. HGF protein bound NRP1 and binding was competed with sNRP1. We cloned a novel mouse sNrp1 isoform from liver and provide evidence that this endogenous angiogenesis inhibitor may regulate VEGF or HGF bioavailability during normal physiological growth and development as well as during liver regeneration.

Address for correspondence: Diane R. Bielenberg, Ph.D., Boston Children's Hospital, 300 Longwood Avenue, Boston, MA 02115; 617-919-2428, diane.bielenberg@childrens.harvard.edu.

Conflict of interest

The authors state that there are no conflicts of interest to disclose.

Keywords

liver; hepatectomy; hepatocyte; endothelial cell; angiogenesis; anti-angiogenesis; neuropilin; VEGF; HGF; development

Introduction

All physiological development and growth is dependent on angiogenesis [1]. Organ expansion requires new capillary growth to nourish the proliferating tissues. VEGF is a potent angiogenic factor capable of stimulating new vessels. Under hypoxia, VEGF is upregulated and recruits new vessels toward the hypoxic area. VEGF stimulates endothelial cell (EC) proliferation, migration and permeability [2]. VEGF is also an endothelial survival factor made constitutively in the adult liver [3].

VEGF-A (hereafter, VEGF) binds two high affinity tyrosine-kinase transmembrane receptors, VEGFR1 and VEGFR2, with most downstream effects attributed to VEGFR2 signaling [4]. VEGF also binds to transmembrane receptors called neuropilins (NRPs). NRP1 and NRP2 bind VEGF and act as co-receptors for VEGFR1 or -2 [5]. NRPs, which can also bind members of the class 3 semaphorin (SEMA3) family of chemorepulsive proteins, have short cytoplasmic domains with no known kinase activity [6]. Sinusoidal EC of the liver express VEGFR1 and VEGFR2; and genetic ablation of VEGFR2 or inhibition of VEGFR2 activity with tyrosine kinase inhibitors impairs liver regeneration [7,8]. Human liver expresses *NRP1* mRNA [5]; and recently, NRP1 protein was detected on human and rat liver EC [9,10]. In contrast, the liver does not express Nrp2 [11].

More recently, it has been suggested that NRP1 may also bind another heparan sulfate binding protein, hepatocyte growth factor (HGF) [12,13]. HGF is secreted as an inactive, single polypeptide and cleaved by serine proteases into a 69-kD alpha chain and a 34-kD beta chain to produce the active, disulfide-linked, heterodimeric HGF protein [14]. HGF binds the c-met tyrosine kinase receptor. Besides its mitogenic activity for hepatocytes [15], HGF is also a potent angiogenesis factor [16]. NRP1-Fc was shown to bind to immobilized HGF in microtiter plates (solid-phase binding) [13]. NRP1 is suggested to act as a co-receptor for HGF/c-met, similar to its function with VEGF/VEGFR [13]. Others suggest that VEGF may signal via NRP1/c-met in tumor cells [17].

Various human NRP1 isoforms have been identified including the full-length receptor (NRP1) that encompasses 17 exons and an alternative receptor that lacks exon 16 [18]. Several smaller soluble isoforms lacking the MAM/c, transmembrane, and cytoplasmic domains of NRP1 were identified. Our group previously isolated two human sNRP1 isoforms, designated s_{12}NRP1 and s_{11}NRP1, indicating they contain intron 12- or intron 11-derived sequences [19,20]. Other human sNRP1 isoforms were subsequently identified: s_{III}NRP1, which lacks exons 10-11, reads into intron 12 and is 551 aa; and s_{IV}NRP1, which lacks exon 11, reads into intron 12 and is 609 aa [21].

The function of the endogenous sNRP1 isoforms is presumably to bind and sequester ligand [19,21]. Specifically, sNRP1 binds $VEGF_{165}$, competes binding of I^{125}-$VEGF_{165}$ to the

surface of EC, and inhibits VEGF-induced phosphorylation of VEGFR2 on EC [19]. Transfection of tumor cells with *sNRP1* results in necrotic and hemorrhagic tumors [19]. Transgenic mice expressing K14-sNRP1 display changes in the vascular architecture and impaired cutaneous vascular permeability [22]. Similarly, sNRP1-Fc monomers inhibit vascular development in a mouse embryo explant model [23].

Although many angiogenesis inhibitors have been used as exogenous anti-angiogenic agents in pre-clinical models, the distribution and regulation of the endogenous proteins are poorly understood. Our previous *in situ* hybridization (ISH) analysis revealed that hepatocytes are the major source of *sNRP1* in the body [19]. To further study the endogenous soluble isoform, we cloned mouse sNrp1. This novel protein is similar to the human sNRP1 in its inclusive a1a2/b1b2 domain structures but differs in its splicing pattern. Herein, we report that sNrp1 is upregulated in the liver at postnatal day 20 and downregulated during liver regeneration. We demonstrate, for the first time, NRP1 binding to HGF on the surface of cells. Our data support the concept that sNrp1 may alter the VEGF or HGF bioavailability *in vivo*.

Materials and methods

Ethics Approval/Mice

C57Bl/6 mice were purchased from Charles River Laboratories. Partial hepatectomies (67%) were performed surgically as described [24]. VEGFLacZ mice [3] were obtained from Dr. Andras Nagy (Toronto, Canada). Mice were maintained under pathogen-free conditions and procedures were performed in accordance with regulations of the National Institutes of Health (NIH), the Association for Assessment and Accreditation of Laboratory Animal Care (AAALAC), and the Institutional Animal Care & Use Committee (IACUC) at Boston Children's Hospital, Boston, MA (annual renewal approval on July 2, 2013).

sNrp1 cloning

Endogenous mouse sNrp1 cDNA was cloned by 3' RACE [25]. Briefly, a 580-bp PCR product was cloned using the TOPO-TA cloning kit (Invitrogen) from mouse liver. The 3' cDNA clone sequence was identified as a truncated *Nrp1* (*sNrp1*) cDNA. The full-length mouse *sNrp1* was amplified from mouse liver cDNA by PCR using primers 5' *Nrp1a* (ATGGAGAGGGGGCTGCCGTT) and 3' *sNrp1* (CAGATAAGTATGTGAGCCCAAGTGC).

IHC

Paraffin sections were de-waxed and rehydrated. Antigens were retrieved by HIER (pH 8). Endogenous peroxidase was quenched with 3% H_2O_2 in methanol. Sections were blocked in blocking reagent (PerkinElmer) and incubated (4°C) in anti-VEGF Ab1 (Lab Vision). Sections were incubated in biotin-conjugated anti-rabbit (Vector) and HRP-conjugated avidin (Vector). Staining was visualized with DAB (Vector) and counterstained with hematoxylin (Sigma).

X-gal staining

For detection of β-galactosidase activity, cryosections from VEGFLacZ mice were fixed in methanol and incubated (37ºC) in X-gal [1 mg/ml X-gal (5-bromo-4-chloro-3-indolyl-b-D-galactopyranoside) in DMSO; 5 mM $K_3Fe(CN)_6$; 5mM $K_4Fe(CN)_6$; 2 mM $MgCl_2$ in PBS; pH 6.5]. Sections were counterstained with Eosin (Sigma).

ISH – oligonucleotide probes

ISH was used to detect human *sNRP1* using an oligonucleotide probe and was performed as described [19]. Sections were dewaxed, rehydrated, and digested with pepsin. Biotinylated probes included: anti-sense *sNRP1*-specific (TTCTGTCACATTTCGTATTTTATTTGATAC), sense, and poly-dT oligonucleotide. Following hybridization, samples were washed with SSC, incubated with alkaline phosphatase-labeled avidin (Dako), and developed in Fast Red (Research Genetics).

ISH – RNA probes

Sections were de-waxed, rehydrated, and digested with proteinase k; then, post-fixed, dehydrated, and air-dried. Anti-sense human NRP1-specific riboprobe and sense probe were synthesized from 750-bp 3'UTR-derived cDNA using a digoxigenin RNA-labeling kit (Roche). Anti-sense mouse *sNrp1* riboprobe and sense probe were created similarly from 300-bp cDNA. Probes were hybridized and washed in SSC. Alkaline phosphatase-labeled anti-digoxigenin and BM Purple (Roche) were used to visualize the reaction.

Northern blot

Polyadenylated mRNA preparation from mouse organs, electrophoresis, blotting, and hybridization were performed as described [5,19]. Probes were labeled with P^{32}-dCTP (New England Nuclear) using RediPrime DNA labeling Kit (GE Healthcare). Probes were generated to mouse *Nrp1* a/CUB, b/factorV/VIII, 3'UTR, and intron 10-derived (soluble specific 300 bp) domains.

Western blot

Lysates of mouse organs were used neat or precipitated with Con A Sepharose (GE Healthcare). Proteins were reduced, resolved with SDS-PAGE, transferred, and blocked with 5% milk. Blots were incubated with anti-mouse Nrp1 (N-terminal) #AF566 (R&D Systems) or rabbit monoclonal anti-mouse Nrp1 (C-terminal) #2621-1 (Epitomics). Membranes were incubated in HRP-linked secondary antibody, washed, and exposed to ECL (PerkinElmer).

HGF binding

Porcine aortic endothelial cells (PAE) and PAE NRP1 cells were grown in Ham's F12 media with 10% FBS as previously described [26]. MDA-MB-231 breast cancer cells (positive control) were obtained from ATCC (HTB26) and cultured in DMEM with 10% FBS. Cells were grown on glass slides and incubated for 30 min on ice in 400 ng biotinylated human HGF (R&D Systems) followed by 30 min in avidin-FITC. Cells were washed twice in RDF1 buffer (R&D Systems) and fixed in 4% PFA. Alternately, cells were incubated for 30 min on

ice in 200 ng biotinylated human HGF or 10:1 (2μg:200ng) mixture of human sNRP1:biotinylated human HGF (both in same volume), incubated in avidin-FITC, washed and fixed as above. Slides were mounted with fluorescent mount and coverslips.

Results

Human sNRP1 versus mouse sNrp1

NRP1 is a transmembrane receptor consisting of 923 aa and an overall aa sequence identity of 93% between human and mouse NRP1. Human and mouse NRP1 have similar domain structures (**Figure 1A**). The largest and most abundant endogenous human soluble NRP1 isoform found in tissues and cells is $s_{12}NRP1$, hereafter called sNRP1 (**Figure 1B**) [19]. This 644 aa soluble receptor is created via alternative splicing and is identical to human NRP1 through the first 12 exons. Its sequence reads into intron 12 and results in an mRNA with a unique 28 bp sequence and a protein ending in 3 novel amino acids (GIK), not found in NRP1 (**Figure 1C**, upper panel). This endogenous sNRP1 protein contains all of the ligand binding domains of NRP1, yet lacks the c domain; therefore, it is likely a monomer.

In order to study the regulation and function of this soluble receptor in greater detail, we turned to a mouse model. We cloned mouse *sNrp1* from mouse liver tissue using 3' RACE. The resulting product had a predicted size of 588 aa and contained the a1a2 and b1b2 ligand binding domains, but lacked all domains 3' of b2 including the b/c-linker, c, transmembrane and cytoplasmic domains (**Figure 1 B-C**, lower panels).

sNrp1 expression in the liver

The distribution of NRP1 and sNRP1 was investigated in human liver sections by ISH. Although NRP1 and sNRP1 are alternatively spliced isoforms of the same gene, their patterns of distribution and localization within the liver were non-overlapping. The full-length *NRP1* mRNA was expressed in EC of veins and sinusoids (**Figure 1D**, purple color) whereas, *sNRP1* mRNA was highly expressed by hepatocytes (**Figure 1E**, pink color). The sense probe for both *NRP1* and *sNRP1* did not show any specific staining (data not shown).

ISH was used to localize mouse *sNrp1* mRNA (**Figure 1F**, purple color). In both human liver and mouse liver, hepatocytes were shown to highly express the soluble isoform (compare **Figure 1E** and **Figure 1F**). Mouse *sNrp1* was abundantly localized in hepatocytes surrounding central veins, and its expression was diminished in hepatocytes more distant from the veins (**Figure 1F**). All hepatocytes had intact mRNA as shown by positive staining using a polydT probe (data not shown).

VEGF expression in the liver

Since the sNrp1 protein contains domains capable of binding VEGF, we also examined the tissue distribution of VEGF protein in sections of adult mouse liver (**Figure 1G**). Using IHC, we determined that the VEGF protein was expressed by mouse hepatocytes in a pattern similar to that of *sNrp1* (compare **Figure 1F** and **G**). VEGF is a secreted protein that can bind heparan sulfate proteoglycans and may be sequestered in the extracellular matrix. Therefore, to confirm that the hepatocytes were indeed the source of the VEGF protein,

adult mouse liver sections from transgenic VEGFLacZ mice [3] were stained with x-gal. Blue nuclei (due to the nuclear translocation signal of the β-gal gene) were detected only in hepatocytes and not in EC (**Figure 1H**).

Comparing the expression of Nrp1 and sNrp1 in mouse organs

We previously compared the expression of full-length *Nrp1* mRNA to *sNrp1* mRNA in various adult mouse organs by northern blot analysis and found that kidney, lung, and brain primarily expressed *Nrp1* mRNA, whereas the liver expressed a smaller mRNA band (presumed to be *sNrp1*) in addition to *Nrp1* [22]. To determine whether the 2 kb band was indeed the same soluble isoform that we had cloned, a northern blot containing mRNA from adult mouse kidney, liver, and heart was serially incubated with probes to the a domain, b domain, intron 10-derived sequence, and *Nrp1* 3' untranslated region (UTR). As expected, the probes to the a and b domains detected both the 7 kb *Nrp1* mRNA and the 2 kb *sNrp1* mRNA (**Figure 2A**, left panels). The intronic probe only hybridized to the 2 kb *sNrp1* band whereas the 3'UTR probe identified only the receptor isoform (**Figure 2A**, right panels). In fact, the liver was the only organ that expressed more soluble than full-length receptor.

To determine whether sNrp1 protein was expressed *in vivo*, western blot analysis was performed. Whole cell protein lysates were isolated from various adult mouse organs and all organs were found to express the full-length Nrp1 receptor protein (130 kD) (**Figure 2B**). Kidney, liver and heart also expressed a smaller protein (sNrp1) detected with neuropilin 1 antibody. To more clearly identify this smaller isoform, protein lysates were concentrated with ConA-sepharose beads (which bind glycoproteins), run on SDS-PAGE, and the western blot was serially incubated with anti-Nrp1 antibodies specific to either the N terminus or the C terminus. Full-length Nrp1 protein (130 kD) was detected in both liver and heart tissue with both antibodies; the soluble isoform was only detected with N-terminal-specific antibodies (**Figure 2C**).

Developmental regulation of sNrp1

Comparing neonatal mouse liver and heart to their mother's (11 week old) liver and heart revealed a dramatic difference in the expression of *sNrp1* mRNA. *sNrp1* was not detected in P3 livers by northern blot analysis (**Figure 2D**). To further examine this apparent age-dependent regulation of *sNrp1*, livers from mice ranging from 2 to 90 days postnatal were examined. Levels of mouse *sNrp1* were dramatically elevated at postnatal day 20 (**Figure 2E**). *sNrp1* expression in kidney was upregulated at similar time points (day 17-20) but to a lesser extent (**Figure 2F**). To determine whether VEGF was expressed in the liver at P17, VEGFLacZ mice were examined by x-gal staining. β-gal expressing hepatocytes confirmed that VEGF was produced at this time point (**Figure 2G**). P20 also coincided with a time point at which mouse body weight and organ weight (heart, liver, and kidney) began to slow or plateau in the mice used for our study (**Figure 3A-D**).

HGF binding to NRP1

The slowing of liver growth around postnatal day 20 (**Figure 3C**) may be do to the direct inhibition of hepatocyte proliferation (via the inhibition of HGF) or the inhibition of angiogenesis (via the inhibition of VEGF or HGF). HGF has been shown to bind to

immobilized NRP1-Fc on plastic but not on cells [13]. PAE cells transfected with human NRP1 bound HGF protein in binding assays (**Figure 3H**), while untransfected PAE cells (negative control) did not (**Figure 3I**). PAE cells may express porcine c-met but cannot bind human HGF due to its species-specific nature [27]. Human breast cancer cells (MDAMB231), which express c-met and NRP1, served as a positive control (**Figure 3G**). Additionally, human sNRP1 (purified a1a2b1b2 domain) [28] inhibited HGF binding to cells when pre-incubated with HGF (**Figure 3J-K**).

sNrp1 and VEGF expression during liver regeneration

The expression of *sNrp1* and VEGF was next examined in a model of liver angiogenesis and regeneration. ISH for *sNrp1* and IHC for VEGF was conducted in sections of adult mouse liver at day 0,1, 3, 5, and 10 following 67% PHx. VEGF protein (brown color) was detected in hepatocytes surrounding veins in normal liver (day 0), and this pattern did not change until day 3 following PHx when VEGF was found in virtually all hepatocytes (**Figure 4B, D, F**). VEGF protein expression remained high at day 4-5 but was decreased dramatically by day 10 (**Figure 4H, J; Figure 3F**). Peri-venous hepatocytes also expressed *sNrp1* (purple) in normal livers (day 0) (**Figure 4A**). *sNrp1* was dramatically downregulated or nearly undetectable on day 1 after PHx (**Figure 4C**) and remained low until day 5 following PHx (**Figure 4G**). The pattern of *sNrp1* on day 5 was similar to normal liver although the signal intensity was slightly stronger. At 10 days after PHx, *sNrp1* was increased above normal levels and its expression was detected in nearly all hepatocytes (**Figure 4I**). The increase in levels of *sNrp1* at day 5 coincided with a plateau in liver weight (**Figure 3E**).

Discussion

The liver is a unique organ with specialized epithelial cells (hepatocytes) and sinusoidal capillaries. Most hepatocytes are in direct contact with a sinusoid. Blood flow in the liver originates from both the hepatic artery and the portal vein and travels through sinusoids to collect in the central veins, which coalesce into the hepatic vein. Oxygenation is highest in zone 1 of the lobule near the triad and lowest in zone 3 near the central vein (**Figure 5**). This oxygen distribution pattern may explain why VEGF is highest in zone 3, which is relatively hypoxic. Although VEGF is a potent inducer of angiogenesis, its constitutive expression by hepatocytes in the normal adult liver, in the absence of angiogenesis, may point to a role as a survival factor, an association that has been documented for fenestrated EC in other tissues [3].

Homeostasis is based upon a balance between stimulatory and inhibitory molecules. Among the VEGF family of receptors, VEGFR1 has a soluble isoform called sFlt-1 [29]. sFlt-1 is associated with pre-eclampsia, a pathology of pregnancy characterized by hypertension and proteinuria [30]. Endogenous sVEGFR2 was cloned from mouse cornea where it functions as a monomer to bind VEGF-A and -C and inhibit lymphangiogenesis [31].

A dichotomy exists in the liver such that NRP1 is found only in EC and sNRP1 only in hepatocytes. Our EC-specific results of NRP1 are in agreement with IHC previously reported [9,10]. NRP1 is typically found in arteries, not veins, during development [32]; yet in the adult liver, NRP1 is expressed on arteries, veins, and capillaries [9]. There is currently no

antibody that can specifically identify only sNRP1 (and not NRP1) as it includes only 3 novel amino acids at its C-terminus.

Similar to human liver, the adult mouse liver expressed Nrp1 mRNA and another band at approximately 2 kb (**Figure 2A**). Using 3' RACE with mouse liver cDNA, a novel isoform of mouse Nrp1 was identified. The *sNrp1* transcript differed in sequence from any of the previously reported soluble isoforms. *sNrp1* (also called $s_{10}Nrp1$ according to the previous convention) is generated from a read-through into intron 10 and contained 300 bp at the 3' end not found in *Nrp1*. An intronic probe confirmed that the 2 kb band found in adult mouse liver corresponded to the cloned sequence. Kidney and heart tissue weakly express *sNrp1*. The sNrp1 protein contains only two novel amino acids. Importantly, sNrp1 contains both VEGF and SEMA3 ligand-binding domains as confirmed by northern blotting with probes specific to each domain. A second soluble Nrp1 isoform is likely as probes to the b domain clearly showed two bands in the region near 2 kb (**Figure 2A**).

Both membrane-bound and soluble Nrp1 proteins were detected in mouse liver using antibodies specific to the N-terminus. As expected, antibodies to Nrp1 C-terminus detected only 130-kD receptor protein. NRP1 protein expression in various tissues and tumors has been examined using IHC [33,34]. In light of our identification of the soluble Nrp isoform, such results must be interpreted with caution when antibodies specific to extracellular epitopes have been used, as this antibody would detect both NRP1 isoforms. Thus, the interpretation of such results may be the opposite when dealing with soluble (antiangiogenic) versus receptor (angiogenic) isoforms.

The expression of *sNrp1* during postnatal mouse development was evaluated. A dramatic upregulation in *sNrp1* was observed in the liver at P20. The mechanism for this upregulation is unclear, but it did correlate with a plateau in the weight of the developing liver. HGF is a potent mitogen and survival factor in the liver [35]. *HGF* mRNA levels increased in the rat postnatally at day 5 and peaked at day 14 [36]. We examined HGF ligand binding to NRP1 on the surface of cells *in vitro*. HGF binding assays on cells are complicated by the fact that most cells also express the c-met tyrosine kinase receptor. However, HGF is species-specific, therefore human HGF binds only to human cells or human receptors [27]. We exploited this fact and used PAE cells as our background or negative control. Even though PAE cells may express porcine c-met, they did not bind human biotinylated HGF. Human NRP1, on the cell surface, did bind HGF (**Figure 3H**). Importantly, sNRP1 could sequester HGF and compete HGF from binding to the cell surface. Thus, we speculate that as the liver reaches its full size, sNrp1 increases to curb growth and angiogenesis by neutralizing HGF and/or VEGF and halting organ growth.

Liver regeneration can be a model to study angiogenesis [35,37]. The process following 67% partial hepatectomy involves massive hepatocyte proliferation (days 1-3), followed by EC proliferation and sprouting (days 3-5), with the total liver mass returning to approximately normal size within 7-10 days [24,38,39]. In our experiments, liver weight nearly doubled in the first 2 days. VEGF protein was elevated in hepatocytes 3-5 days after PHx. These data are consistent with other studies of VEGF expression during regeneration [38,39]. IHC localization of VEGF suggested alterations in its localization during regeneration with VEGF initially

found in peri-venous hepatocytes (day 0-1), then in nearly all hepatocytes (days 3-5), and finally widely distributed at low levels (day 10).

Like VEGF, sNrp1 was constitutively expressed around central veins in normal liver. Unlike its ligand, sNrp1 was dramatically downregulated immediately following PHx, remained low until day five and elevated above normal levels by 10 days (**Figure 4**). Taken together, our studies suggest that sNrp1 levels in the liver are low during times of active angiogenesis such as during the growth phase of the neonate (P1-20) or during the proliferative stage following hepatectomy (d1-5). sNrp1 may act as an endogenous angiogenesis inhibitor as it is expressed at higher levels at times when growth is slowed, which would be expected to be associated with reduced VEGF signaling.

EGF dramatically upregulates NRP1 and sNRP1 in epithelial cells and tumor cells [40]. Therefore, it is surprising that mouse sNrp1, which shares the same promoter as Nrp1, would be downregulated in the liver one day after hepatectomy when TGFα/EGF levels are known to be elevated [41]. This suggests that another factor may be responsible for inhibiting sNrp1 or that EGFR ligands may not regulate Nrp1 in hepatocytes.

We have shown that human sNRP1 binds VEGF, inhibits VEGF binding to EC, and inhibits the activation of VEGFR2 by VEGF on EC [19]. Since mouse sNrp1 contains the same ligand binding domains as human sNRP1, it is reasonable to assume that sNrp1 in the mouse liver also sequesters VEGF, thereby acting to inhibit VEGF-induced neovascularization. sNrp1 is expected to bind and sequester not only VEGF but also other Nrp1 ligands including PlGF, VEGF-B, and SEMA3A. PlGF, an angiogenic ligand, is upregulated after PHx [42]; whereas SEMA3A, an anti-angiogenic ligand, is significantly downregulated during the first 6 days following PHx [10].

Although knocking-out sNRP1 in the liver would be useful to confirm our strong correlative results shown here, such efforts are likely to lead to ambiguous outcomes. As mentioned, *Nrp1* and *sNrp1* both arise from the same gene—therefore, knocking-out sNrp1 would also deplete the Nrp1 receptor in the liver. Additionally, Nrp1 KO mice die at E12.5-13.5 with severe vascular defects [43].

Endogenous angiogenesis inhibitors have been shown to be expressed by specific tissues. For example, both sFlt1 and sVEGFR2 are expressed in the cornea where they functions to maintain the tissue in an avascular state [31,44]. By comparison, we conclude that sNrp1 is an endogenous angiogenesis inhibitor secreted by hepatocytes to sequester its ligands and control the balance of angiogenesis. sNrp1 protein (or specifically peptides including the b domain region) may be useful for the management of a variety of angiogenesis-related diseases including arthritis, various proliferative retinopathies, hemangiomas, and cancer.

Acknowledgements

References

1. Folkman J. Angiogenesis: an organizing principle for drug discovery? Nat Rev Drug Discov. 2007; 6:273–286. [PubMed: 17396134]

2. Brown LF, Detmar M, Claffey K, et al. Vascular permeability factor/vascular endothelial growth factor: a multifunctional angiogenic cytokine. Exs. 1997; 79:233–269. [PubMed: 9002222]

3. Maharaj AS, Saint-Geniez M, Maldonado AE, et al. Vascular endothelial growth factor localization in the adult. Am J Pathol. 2006; 168:639–648. [PubMed: 16436677]

4. Shibuya M, Claesson-Welsh L. Signal transduction by VEGF receptors in regulation of angiogenesis and lymphangiogenesis. Exp Cell Res. 2006; 312:549–560. [PubMed: 16336962]

5. Soker S, Takashima S, Miao HQ, et al. Neuropilin-1 is expressed by endothelial and tumor cells as an isoform-specific receptor for vascular endothelial growth factor. Cell. 1998; 92:735–745. [PubMed: 9529250]

6. Bielenberg DR, Klagsbrun M. Targeting endothelial and tumor cells with semaphorins. Cancer Metastasis Rev. 2007; 26:421–431. [PubMed: 17768598]

7. Ding BS, Nolan DJ, Butler JM, et al. Inductive angiocrine signals from sinusoidal endothelium are required for liver regeneration. Nature. 2010; 468:310–315. [PubMed: 21068842]

8. Hora C, Romanque P, Dufour JF. Effect of sorafenib on murine liver regeneration. Hepatology. 2011; 53:577–586. [PubMed: 21274878]

9. Berge M, Allanic D, Bonnin P, et al. Neuropilin-1 is upregulated in hepatocellular carcinoma and contributes to tumour growth and vascular remodelling. J Hepatol. 2011; 55:866–875. [PubMed: 21338642]

10. Fu LKT, Iwabuchi K, Ichinose S, Yanagida M, Ogawa H, Watanabe S, Maruyama T, Suyama M, Takamori K. Interplay of neuropilin-1 and semaphorin 3A after partial hepatectomy in rats. World J Gastroenterol. 2012; 18:5034–5041. [PubMed: 23049211]

11. Bielenberg DR, Seth A, Shimizu A, et al. Increased Smooth Muscle Contractility in Mice Deficient for Neuropilin 2. Am J Pathol. 2012; 181:548–559. [PubMed: 22688055]

12. West DC, Rees CG, Duchesne L, et al. Interactions of multiple heparin binding growth factors with neuropilin-1 and potentiation of the activity of fibroblast growth factor-2. The Journal of biological chemistry. 2005; 280:13457–13464. [PubMed: 15695515]

13. Sulpice E, Plouet J, Berge M, et al. Neuropilin-1 and neuropilin-2 act as coreceptors, potentiating proangiogenic activity. Blood. 2008; 111:2036–2045. [PubMed: 18065694]

14. Mizuno K, Nakamura T. Molecular characteristics of HGF and the gene, and its biochemical aspects. Exs. 1993; 65:1–29. [PubMed: 8422543]

15. Matsumoto K, Nakamura T. Hepatocyte growth factor: molecular structure and implications for a central role in liver regeneration. Journal of gastroenterology and hepatology. 1991; 6:509–519. [PubMed: 1834243]

16. Aoki M, Morishita R, Taniyama Y, Kaneda Y, Ogihara T. Therapeutic angiogenesis induced by hepatocyte growth factor: potential gene therapy for ischemic diseases. Journal of atherosclerosis and thrombosis. 2000; 7:71–76. [PubMed: 11426585]

17. Zhang S, et al. Vascular endothelial growth factor regulates myeloid cell leukemia-1 expression through neuropilin-1-dependent activation of c-MET signaling in human prostate cancer cells. Molecular cancer. 2010; 9:9. [PubMed: 20085644]

18. Tao Q, Spring SC, Terman BI. Characterization of a new alternatively spliced neuropilin-1 isoform. Angiogenesis. 2003; 6:39–45. [PubMed: 14517403]

19. Gagnon ML, Bielenberg DR, Gechtman Z, et al. Identification of a natural soluble neuropilin-1 that binds vascular endothelial growth factor: In vivo expression and antitumor activity. Proc Natl Acad Sci U S A. 2000; 97:2573–2578. [PubMed: 10688880]

20. Rossignol M, Gagnon ML, Klagsbrun M. Genomic organization of human neuropilin-1 and neuropilin-2 genes: identification and distribution of splice variants and soluble isoforms. Genomics. 2000; 70:211–222. [PubMed: 11112349]

21. Cackowski FC, Xu L, Hu B, et al. Identification of two novel alternatively spliced Neuropilin-1 isoforms. Genomics. 2004; 84:82–94. [PubMed: 15203206]

22. Mamluk R, Klagsbrun M, Detmar M, et al. Soluble neuropilin targeted to the skin inhibits vascular permeability. Angiogenesis. 2005; 8:217–227. [PubMed: 16328161]

23. Yamada Y, Takakura N, Yasue H, et al. Exogenous clustered neuropilin 1 enhances vasculogenesis and angiogenesis. Blood. 2001; 97:1671–1678. [PubMed: 11238106]

24. Greene AK, Puder M. Partial hepatectomy in the mouse: technique and perioperative management. J Invest Surg. 2003; 16:99–102. [PubMed: 12746193]

25. Bates D, Taylor GI, Minichiello J, et al. Neurovascular congruence results from a shared patterning mechanism that utilizes Semaphorin3A and Neuropilin-1. Dev Biol. 2003; 255:77–98. [PubMed: 12618135]

26. Bielenberg DR, Hida Y, Shimizu A, et al. Semaphorin 3F, a chemorepulsant for endothelial cells, induces a poorly vascularized, encapsulated, nonmetastatic tumor phenotype. The Journal of clinical investigation. 2004; 114:1260–1271. [PubMed: 15520858]

27. Francone TD, Landmann RG, Chen CT, et al. Novel xenograft model expressing human hepatocyte growth factor shows ligand-dependent growth of c-Met-expressing tumors. Molecular cancer therapeutics. 2007; 6:1460–1466. [PubMed: 17431125]

28. Mamluk R, Gechtman Z, Kutcher ME, et al. Neuropilin-1 binds vascular endothelial growth factor 165, placenta growth factor-2, and heparin via its b1b2 domain. The Journal of biological chemistry. 2002; 277:24818–24825. [PubMed: 11986311]

29. Kendall RL, Thomas KA. Inhibition of vascular endothelial cell growth factor activity by an endogenously encoded soluble receptor. Proc Natl Acad Sci U S A. 1993; 90:10705–10709. [PubMed: 8248162]

30. Baumwell S, Karumanchi SA. Pre-eclampsia: clinical manifestations and molecular mechanisms. Nephron Clin Pract. 2007; 106:c72–81. [PubMed: 17570933]

31. Albuquerque RJ, Hayashi T, Cho WG, et al. Alternatively spliced vascular endothelial growth factor receptor-2 is an essential endogenous inhibitor of lymphatic vessel growth. Nat Med. 2009; 15:1023–1030. [PubMed: 19668192]

32. Herzog Y, Kalcheim C, Kahane N, et al. Differential expression of neuropilin-1 and neuropilin-2 in arteries and veins. Mech Dev. 2001; 109:115–119. [PubMed: 11677062]

33. Jubb AM, Strickland LA, Liu SD, et al. Neuropilin-1 expression in cancer and development. J Pathol. 2012; 226:50–60. [PubMed: 22025255]

34. Hansel DE, Wilentz RE, Yeo CJ, et al. Expression of neuropilin-1 in high-grade dysplasia, invasive cancer, and metastases of the human gastrointestinal tract. Am J Surg Pathol. 2004; 28:347–356. [PubMed: 15104297]

35. Jia C. Advances in the regulation of liver regeneration. Expert review of gastroenterology & hepatology. 2011; 5:105–121. [PubMed: 21309676]

36. Kagoshima M, Kinoshita T, Matsumoto K, Nakamura T. Developmental changes in hepatocyte growth factor mRNA and its receptor in rat liver, kidney and lung. European journal of biochemistry / FEBS. 1992; 210:375–380. [PubMed: 1332867]

37. Fausto N, Campbell JS, Riehle KJ. Liver regeneration. Hepatology. 2006; 43:S45–53. [PubMed: 16447274]

38. Yoshida D, Akahoshi T, Kawanaka H, et al. Roles of vascular endothelial growth factor and endothelial nitric oxide synthase during revascularization and regeneration after partial hepatectomy in a rat model. Surg Today. 2011; 41:1622–1629. [PubMed: 21969195]

39. Taniguchi E, Sakisaka S, Matsuo K, et al. Expression and role of vascular endothelial growth factor in liver regeneration after partial hepatectomy in rats. J Histochem Cytochem. 2001; 49:121–130. [PubMed: 11118484]

40. Parikh AA, Fan F, Liu WB, et al. Neuropilin-1 in human colon cancer: expression, regulation, and role in induction of angiogenesis. Am J Pathol. 2004; 164:2139–2151. [PubMed: 15161648]

41. Stromblad S, Andersson G. The coupling between transforming growth factor-alpha and the epidermal growth factor receptor during rat liver regeneration. Exp Cell Res. 1993; 204:321–328. [PubMed: 8440328]

42. Vanheule E, Fan YD, Van Huysse J, et al. Expression of placental growth factor in regenerating livers after partial hepatectomy in the rat. Eur J Gastroenterol Hepatol. 2011; 23:66–75. [PubMed: 21088600]

43. Kawasaki TKT, Bekku Y, Matsuda Y, Sanbo M, Yagi T, Fujisawa H. A requirement for neuropilin-1 in embryonic vessel formation. Development. 1999; 126:4895–4902. [PubMed: 10518505]

44. Sela S, Itin A, Natanson-Yaron S, et al. A novel human-specific soluble vascular endothelial growth factor receptor 1: cell-type-specific splicing and implications to vascular endothelial growth factor homeostasis and preeclampsia. Circ Res. 2008; 102:1566–1574. [PubMed: 18515749]

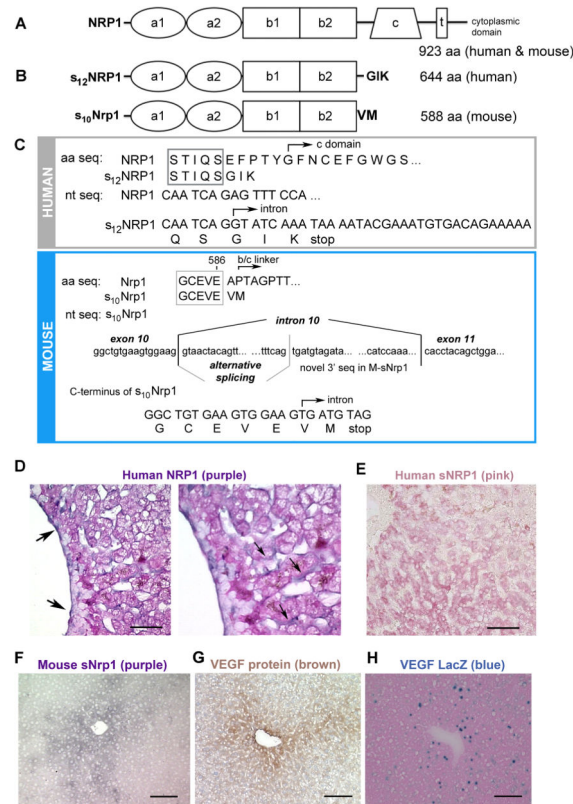**Figure 1. Comparison of human and mouse Neuropilin 1 isoforms**
(**A**) Diagram of human and mouse NRP1 structure. (**B**) Upper panel: diagram of human
s_{12}NRP1. Lower panel: diagram of mouse s_{10}Nrp1. (**C**) Upper panel: Human sNRP1 ends in
3 novel aa (GIK). Lower panel: The novel mouse sNrp1 reads through into intron 10, has an
alternatively spliced region, and 300 unique nt encoding 2 novel aa (VM) and a stop codon.
(**D**) ISH demonstrates human *NRP1* (purple color) in EC (arrows) of sinusoids and veins.
Eosin counterstain (pink color). Scale bar = 30 μm. Right panel is magnification of left
panel. (**E**) ISH demonstrates human *sNRP1* (pink color) in hepatocytes. Scale bar = 50 μm.
(**F**) ISH demonstrates mouse *sNrp1* (purple color) in hepatocytes surrounding central veins.
(**G**) IHC for VEGF protein (brown color) in hepatocytes surrounding central veins.
Hematoxylin counterstain (blue nuclei). (**H**) X-gal staining demonstrates LacZ signal (blue
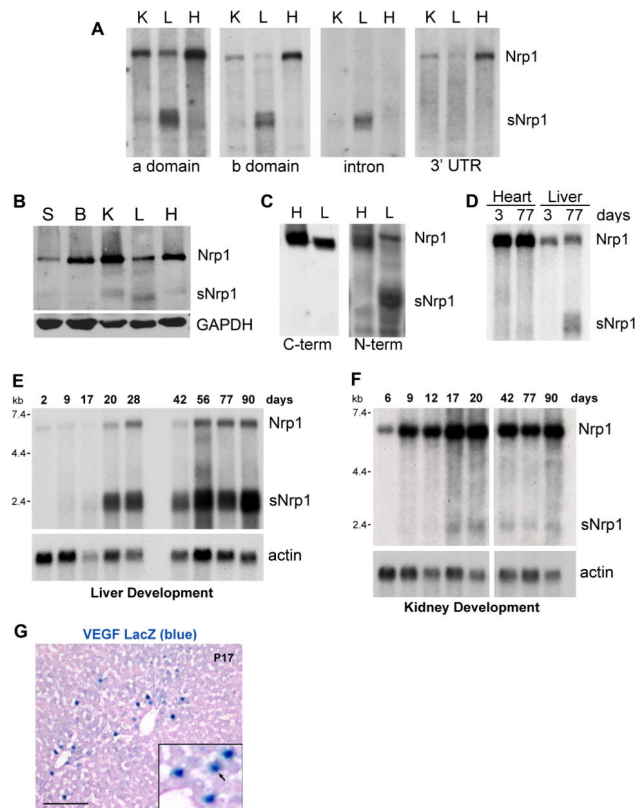color) in hepatocytes. Eosin counterstain (pink color). Scale bars F-H = 0.1 mm.

Figure 2. *sNrp1* mRNA and protein is expressed in the adult liver

(A) Northern blot. *sNrp1* is detected with a, b, and intron probes in the liver (L); while *Nrp1* is detected with a, b, and 3'UTR probes in kidney (K), liver, and heart (H). **(B)** Western blot of mouse organs. GAPDH = loading control. Skin (S), Brain (B). **(C)** Western blot. N-terminal anti-Nrp1 detects Nrp1 in adult liver and heart and sNrp1 in liver. C-terminal anti-Nrp1 detects Nrp1 in heart and liver. **(D)** Northern blot. *Nrp1* mRNA in adult and neonatal (P3) heart and liver. *sNrp1* in the adult liver. **(E)** *sNrp1* is upregulated in P20 livers and remains elevated. **(F)** *sNrp1* is slightly upregulated in P17-20 kidneys. *Nrp1* is more abundant than *sNrp1* in kidney. Actin = loading control. **(G)** VEGF (blue nuclei) in P17 VEGFLacZ mouse liver. Eosin counterstain. Scale bar = 0.1 mm.
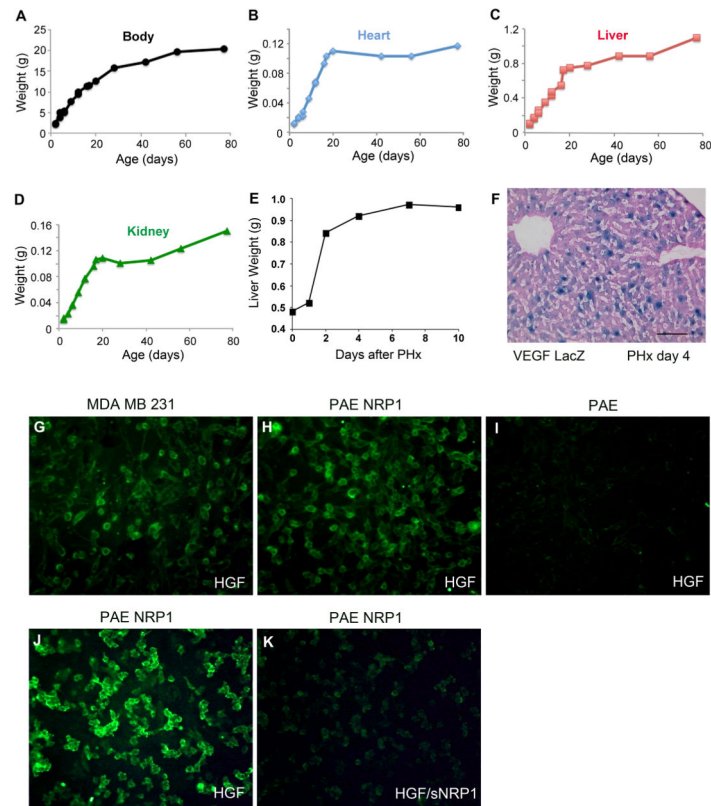
Figure 3. NRP1 binds HGF

The weight of the overall mouse **(A)**, heart **(B)**, liver **(C)**, and kidney **(D)** were measured at various time points after birth. All weights plateaued around 20 days. **(E)** Graph of liver weight following PHx. **(F)** VEGF (blue nuclei) is expressed in many hepatocytes 4 days following PHx. Eosin counterstain. Scale bar = 0.1 mm. **(G-K)** HGF binding assay using biotinylated human HGF and avidin-FITC. HGF binds MDAMB231 cells **(G)** and PAE NRP1 cells **(H, J)**, but not PAE cells **(I)**. sNRP1 competes the binding of HGF to NRP1 **(K)**. Note green color is on the cell membrane.
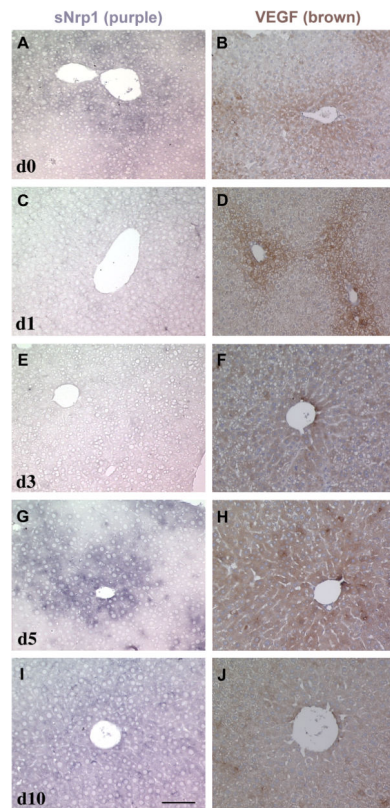
Figure 4. Expression and regulation of *sNrp1* and VEGF following PHx (days 0-10)
ISH for *sNrp1* (**A, C, E, G, I**) and IHC for VEGF (**B, D, F, H, J**) after 67% PHx. Day 0 (**A, B**), day 1 (**C, D**), day 3 (**E, F**), day 5 (**G, H**), day 10 (**I, J**) after PHx. By day 3, *sNrp1* is downregulated and VEGF is upregulated.
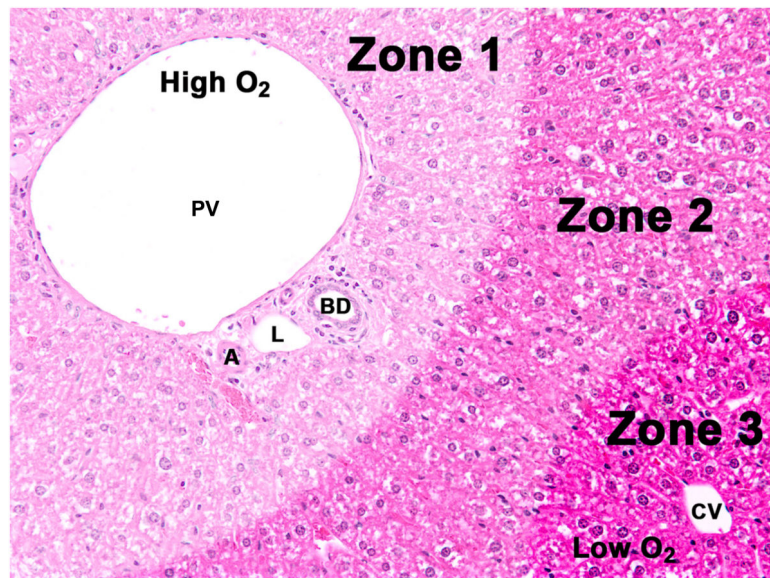
Figure 5. Diagram of liver

Oxygenation (O_2) is highest in zone 1 near the portal vein (PV), artery (A), and bile duct (BD) (triad) and lowest near the central vein (CV). L, lymphatic. Image was false-colored to depict the relative zones.